# UC Santa Barbara

## UC Santa Barbara Previously Published Works

### Title

Mercury species induce metabolic reprogramming in freshwater diatom Cyclotella meneghiniana

### Permalink

https://escholarship.org/uc/item/7jd026dm

### Authors

Santos, João P

Li, Weiwei

Keller, Arturo A

et al.

### Publication Date

2024-03-01

### DOI

10.1016/j.jhazmat.2023.133245

### Copyright Information

This work is made available under the terms of a Creative Commons Attribution License, available at https://creativecommons.org/licenses/by/4.0/

Peer reviewed

eScholarship.org Powered by the California Digital Library
University of California

Journal of Hazardous Materials 465 (2024) 133245

Contents lists available at ScienceDirect

Journal of Hazardous Materials

journal homepage: www.elsevier.com/locate/jhazmat

# Mercury species induce metabolic reprogramming in freshwater diatom *Cyclotella meneghiniana*

João P. Santos [a,*,1], Weiwei Li [b], Arturo A. Keller [b,2], Vera I. Slaveykova [a,*,3]

[a] University of Geneva, Faculty of Sciences, Earth and Environment Sciences, Department F.-A. Forel for Environmental and Aquatic Sciences, Environmental Biogeochemistry and Ecotoxicology, 66 Blvd Carl-Vogt, CH 1211 Geneva, Switzerland
[b] Bren School of Environmental Science & Management, University of California, Santa Barbara, CA 93106-5131, United States

## HIGHLIGHTS

- Diatom metabolic reprogramming is induced by short-term exposure to sub-lethal Hg(II) and MeHg concentrations.
- Hg(II) exposure induces ROS generation, membrane integrity and chlorophyll depletion.
- MeHg triggers a GSH antioxidant response that is evident at the physiological and metabolic levels.
- Hg(II) and MeHg affected amino acids, nucleotides, fatty and carboxylic acids, and antioxidant metabolism.
- At equivalent Hg cellular concentrations, MeHg alters diatom metabolism stronger than Hg(II).

## GRAPHICAL ABSTRACT

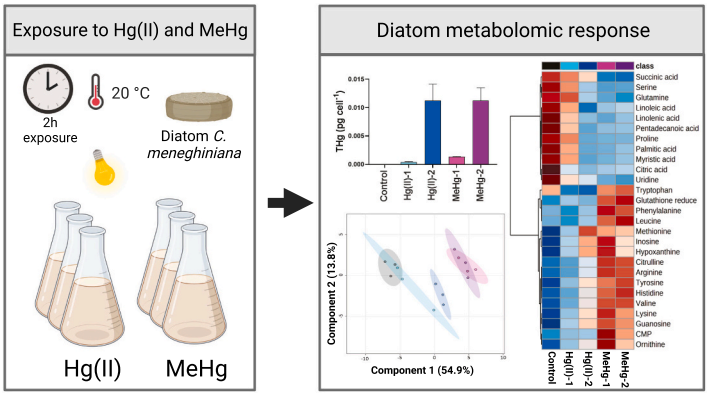


## ARTICLE INFO

Editor: Nan Sang

*Keywords:*
Inorganic mercury
Methylmercury
Bioaccumulation
Metabolomics
Physiological endpoints
Diatom

## ABSTRACT

Mercury is a hazardous pollutant of global concern. While advances have been made in identifying the detrimental effects caused by Hg species in phytoplankton, knowledge gaps remain regarding the metabolomic perturbations induced by inorganic mercury (Hg(II)) and monomethylmercury (MeHg) in these organisms. Diatoms represent a major phytoplankton group essential in various global biogeochemical cycles. The current study combined targeted metabolomics, bioaccumulation, and physiological response assays to investigate metabolic perturbations in diatom *Cyclotella meneghiniana* exposed for 2 h to nanomolar concentrations of Hg(II) and MeHg. Our findings highlight that such exposures induce reprogramming of the metabolism of amino acids, nucleotides, fatty acids, carboxylic acids and antioxidants. These alterations were primarily mercury-species dependent. MeHg exposure induced more pronounced reprogramming of the metabolism of diatoms than Hg (II), which led to less pronounced effects on ROS generation, membrane permeability and chlorophyll concentrations. Hg(II) treatments presented distinct physiological responses, with more robust metabolic perturbations

* Corresponding authors.
*E-mail addresses:* joao.rodriguespereirasantos@unige.ch (J.P. Santos), vera.slaveykova@unige.ch (V.I. Slaveykova).
[1] ORCID ID 0000-0002-1899-2226
[2] ORCID ID 0000-0002-7638-662X
[3] ORCID ID 0000-0002-8361-2509

https://doi.org/10.1016/j.jhazmat.2023.133245
Received 11 July 2023; Received in revised form 6 December 2023; Accepted 10 December 2023
Available online 13 December 2023
0304-3894/© 2023 The Author(s). Published by Elsevier B.V. This is an open access article under the CC BY license (http://creativecommons.org/licenses/by/4.0/).

at higher exposures. The present study provides first-time insights into the main metabolic alterations in diatom *C. meneghiniana* during short-term exposure to Hg species, deepening our understanding of the molecular basis of these perturbations.

## 1. Introduction

Mercury occurs naturally in the environment, however, anthropogenic activities, mainly since the industrial revolution, have promoted a rise in global Hg emissions and cycling, and consequently, an increase in its concentrations in environmental compartments [1–3]. Mercury continues to be released by industrial activities. For instance, artisanal small-scale gold mining account for 37% of Hg emissions and contamination [4]. Additionally, the global electronic waste (e-waste) industry is estimated to release approximately 50 tons of mercury annually [5,6], further contributing to the increase of Hg contamination.

In the aquatic environment, the two prevailing mercury species - inorganic mercury (Hg(II)) and methylmercury ($CH_3Hg^+$, MeHg) - accumulate in aquatic organisms, and MeHg biomagnifies along food webs, thus presenting a threat to higher-level consumers, including humans [7,8]. Increasing research on Hg species uptake [9,10] and its detrimental effects on primary producers (e.g. diatoms and green algae) revealed that high concentrations of Hg(II) and MeHg induced growth rate inhibition, generation of reactive oxygen species (ROS), influence on plasma membrane permeability, chlorophyll degradation among others [11,12]. However, such physiological endpoints can only partially explain the underlying toxicity mechanisms [13].

Advances in omics techniques, such as metabolomics, are increasingly employed to assess particular chemical stressor-induced metabolic perturbations, understand the mode of action, and provide information before physiological effects [14]. Indeed, metabolomic studies have enabled a mechanistic understanding of the metabolomic perturbations in various phytoplankton species. For instance, increasing Cu levels induced different physiological and cellular metabolic responses in *T. flocculosa* and *S. quadricauda,* leading to fatty acids (FA), glutathione and glutathione S-transferase increase as a possible detoxification response, and cells entering a metabolic restructuring by changing amino acids (AA), FA and sugar concentrations [15,16]. Additionally, Zhang, et al. [17] found that Cu and Cd co-exposure leads to a synergetic effect inducing membrane degradation, oxidative stress, and photosynthesis inhibition. Qu, et al. [18] demonstrated inhibition of the phosphorous assimilation in green alga *Chlorella vulgaris* after exposure to AgNPs due to the dysregulated inositol phosphate metabolism, phosphatidylinositol signaling system and glutathione metabolism. Liu, et al. [19] revealed that dissolved Ag and AgNPs affect the AA metabolism, tricarboxylic acid (TCA) cycle, FA, photosynthesis, photorespiration and oxidative stress the golden-brown alga *Poterioochromonas malhamensis* in a time-dependent manner. Similarly, Liu, et al. [20] showed that the exposure of *C. reinhardtii* to $TiO_2$ with primary size of 5, 15 and 20 nm resulted in perturbation of the similar metabolism pathways except for photosynthesis.

Recently, two pioneering studies have investigated the impact of different mercury species (Hg(II) and MeHg) on the metabolome of *Euglena gracilis* and *Chlamydomonas reinhardtii* [21,22]. An increasing abundance of 21 AA, alteration of the nucleotide metabolism, photorespiration and TCA cycle, as well as the metabolism of FA, carbohydrates and antioxidants, were found in *C. reinhardtii* exposed to both Hg (II) and MeHg [22]. While cysteine, glutathione, and trisaccharide were significantly accumulated in the *E. gracilis* exposed to Hg(II) compared to untreated cultures [21]. Nevertheless, there is still a considerable lack of knowledge concerning the metabolomic alterations induced by either Hg(II) or MeHg on phytoplankton, even though these organisms play a pivotal role in global biogeochemical cycles and food web dynamics.

Diatoms, a major representative of phytoplankton groups, are ubiquitous in freshwater and marine environments [23]. They are significant ecological contributors to ecosystem functioning, accounting for approximately 25% of the world's turnover of silica [24] and potentially responsible for sequestering 20% of the global $CO_2$ in the form of lipids (e.g. triacylglycerols) and carbohydrates (e.g. chrysolaminarin) [25]. Despite diatoms being recognized as an indicator group for water quality assessment and a mandatory group for monitoring under the Water Framework Directive [26,27], their metabolite profiling in response to Hg(II) or MeHg exposure remains unexplored. Therefore, improving this knowledge gap is essential for understanding diatom cellular responses to potential fluctuations in environmental Hg species concentrations and the subsequent impact on the dynamics of Hg-contaminated ecosystems.

The present study aims to obtain insights into the physiological and metabolic alterations of diatom *Cyclotella meneghiniana* during short-term exposure to sub-lethal concentrations of Hg(II) and MeHg. By employing targeted metabolomics, we address the following research questions: (i) what are the major metabolic pathways affected by Hg(II) and MeHg?; (ii) do perturbations in the metabolic pathways exhibit a concentration-dependent response?; (iii) are the perturbations similar or different for Hg(II) and MeHg?

## 2. Material and methods

### 2.1. Material cleaning procedure

All glassware was soaked in nitric acid 10% ($HNO_3$, pro-analysis, Merck, Darmstadt, Germany) and hydrochloric acid 10% (HCl pro-analysis, Merck) baths for 1 h with sonication. The glassware was rinsed with ultrapure water (Milli-Q Direct 8, Merck) and then pyrolyzed for 1 h at 550 °C. After pyrolysis, all material was autoclaved (30 min, 121 °C and 1 bar, LVSA 50/70, Zirbus Technology, Germany).

### 2.2. Cultivation of diatom Cyclotella meneghiniana, biological assays and Hg speciation

Diatom *C. meneghiniana* (CCAC 0036 strain, Collection of Algal Cultures, University of Duisburg-Essen, Germany) was grown in synthetic freshwater medium (SFM, composition in Table S1) at 20 °C with a light intensity of 100 μmol photons $m^{-2}$ $s^{-1}$ and a light:dark regime of 14:10 h. Cultures were maintained inside a culture incubator (Fitotron, model SGC120, Weiss Technik UK Ltd., Loughborough, UK) with a continuous air supply (~150 mL $min^{-1}$) filtered through a capsule filter (0.2 μm Aervent®). All experiments were initiated at the same time of the day, considering the dependence of the algal metabolic state of the growth phase and light exposure [28]. The diatom cells in the mid-exponential growth phase were harvested by mild centrifugation (4062 g, 20 °C, 10 min), rinsed, and re-suspended in simplified SFM (exposure medium, Table S1) to a final cell density of (1.05 ± 0.07) × $10^6$ cells $mL^{-1}$, as determined by flow cytometry (FCM, BD Accuri C6, BD Biosciences, Allschwil, Switzerland).

A total of five different conditions were tested. The first condition consisted of cells unexposed to mercury, serving as the control treatment. The other four conditions included exposing diatom cells to two sub-lethal concentrations of Hg(II) and MeHg. While the selected concentrations exceed those found in the natural environments, they are relevant for contaminated environments, where concentrations have been observed to range from approximately 0.8 - 150 × $10^{-9}$ M [4,6,29]. Furthermore, these concentrations corresponded to a growth inhibition of 20–40% in *C. meneghiniana* cells over a 48 h exposure (Fig. S1). The short-term exposure was chosen to target early-response metabolites to Hg(II) and MeHg, before the emergence of a more general stress

response. Diatom growth was not affected during the 2 h exposure assays. The measured concentrations in the exposure medium containing cells were (8.3 ± 0.44) × $10^{-9}$ M (Hg(II)−1), (6.5 ± 0.69) × $10^{-9}$ M (MeHg−1), (84 ± 0.51) × $10^{-9}$ M (Hg(II)−2) and (79 ± 3.3) × $10^{-9}$ M (MeHg−2) (Table S2). The speciation of Hg(II) and MeHg in the exposure medium was modeled using Visual Minteq (Version 3.2, Table S3). Briefly, parameters comprised 20 °C, pH = 7.0, macronutrients described in Table S1, and Hg species added described in Table S2. For both Hg(II) exposures, > 99.8% of Hg was in the form of $Hg(OH)_2$, while for both MeHg exposures, > 99.5% of MeHg was in the form of $(CH_3Hg)_2OH^+$.

After 2 h of exposure, mercury uptake, physiological endpoints, and metabolic perturbations caused by Hg species were assessed in detail below.

### 2.3. Mercury uptake in C. meneghiniana exposed to Hg(II) and MeHg

The uptake of Hg(II) and MeHg by diatom *C. meneghiniana* was determined by measuring the cellular concentration of total mercury (THg) since, in these cells, the potential for demethylation transformation was found to be negligible (with only approximately 0.17% observed during a 2-hour exposure) and no methylation of Hg(II) detected [30]. Briefly, 45 mL of diatom suspension was collected, centrifuged (4062 g, 4 °C, 10 min), rinsed with Hg-free exposure medium to remove the loosely bound mercury from the diatom surface and then digested in ultrapure $HNO_3$ (65% w/w, EMSURE®; Merk Millipore, Germany) at 85 °C during 12 h as described in Santos, et al. [31]. THg concentrations in the digested cells and exposure medium were measured using a MERX® Automated Total Mercury Analytical System (Brooks Rand Instruments, Seattle, WA, USA). The instrumental linear working range of MERX-T is between 0.08 and 400 ng/L. Linearity was assessed over the range of 20 to 10,000 pg of the analyte mass by constructing a calibration curve (Fig. S2) with seven standard concentrations. Each standard was analyzed at least twice. The calibration curve was plotted and displayed a 99% confidence level ($R^2$ > 0.99). All accepted values met the quality control acceptance criteria defined by US EPA method 1631 [32]. The limit of detection (LOD) of the method is 0.0014 ng $g^{-1}$ and the limit of quantitation (LOQ) of 0.0044 ng $g^{-1}$, as previously described [31]. The accuracy of the measurements was checked by analyzing certified reference material of unicellular microalga *Scenedesmus obliquus* (IAEA-450). The recovery efficiency was 93.6 ± 5.0%. Statistical analysis of the results was assessed using a student's t-test in the GraphPad Prism 9 (GraphPad Software, Inc., La Jolla, CA, USA).

### 2.4. Physiological effects of Hg(II) and MeHg in C. meneghiniana

The physiological responses of *C. meneghiniana* to Hg(II) and MeHg were characterized by determining the generation of cellular reactive oxygen species (ROS), the alterations in membrane integrity, and total chlorophyll and carotenoid concentrations. Unexposed diatoms were used as a negative control.

Cellular ROS levels were determined by FCM (FL1 channel) after staining the cells with 1 μM CellROX® Green reagent (Thermo Fisher Scientific, Waltham, MA, USA) in the dark [12]. Diatoms exposed to 1 × $10^{-4}$ M $H_2O_2$ for 30 min prior to staining with CellROX® Green were used as a positive control. Membrane integrity was also assessed by FCM (FL2 channel) after 30-min incubation with 7 × $10^{-6}$ M propidium iodide (PI, Acros Organics, Geel, Belgium) in the dark [12]. Diatoms treated at 90 °C for 15 min were used as a positive control for PI detection.

Total chlorophyll and carotenoid concentrations were quantified following previously published procedures [33,34]. Briefly, fresh diatom material was collected after exposure and sonicated for 1 min in ice cold bath. Next, the pigments were extracted at 4 °C in the dark for 24 h by incubating diatom pellets in 90% acetone (v/v) and in 100% methanol for measurement of the total chlorophyll and carotenoid concentrations, respectively. The absorbance of the cellular extracts was measured by spectrophotometry (Lambda 365 spectrophotometer, PerkinElmer, Waltham, MA) at wavelengths corresponding to the maximum absorption of the selected pigments and applying the equations with the molar extinction coefficient of the pigments [33,34]. Physiological results were analyzed using parametric statistical test one-way ANOVA followed by the Tukey Kramer HSD test in GraphPad Prism 9 software.

### 2.5. Liquid chromatography - mass spectrometry (LC-MS) targeted metabolomics

At the end of the exposure, the cells were collected and placed in liquid nitrogen to stop metabolic activity, then transferred to − 80 ℃ for 24 h and freeze-dried (Beta 1–8 LSCplus, Christ®, Martin Christ Gefriertrocknungsanlagen GmbH, Germany). Metabolites, including antioxidants, AA, organic acids/phenolics, nucleobase/side/tide, sugar/sugar alcohols and FA, were extracted in 80% methanol containing 2% formic acid, following a previously developed methodology [19,20,22]. Targeted analysis of these metabolites was performed using an Agilent 6470 liquid chromatography triple quadrupole mass spectrometer according to previously established methods [20,35]. The MS parameters are provided in Table S4**.** Of the 82 metabolites analyzed, 40 were found above their detection limits and present in all samples.

Statistical analysis of the targeted metabolomic data was performed using MetaboAnalyst 5.0 [36]. Metabolite concentrations were first adjusted using the batch effect correction function (Table S5). Data were normalized using the probabilistic quotient normalization by the unexposed control treatment and auto-scaled as described in Xia and Wishart [37]. One-way analysis of variance (ANOVA) followed by Fisher's LSD post-hoc analysis with $p < 0.05$ was performed to identify the metabolites differing between Hg(II) and MeHg exposure at different concentrations and control (Table S6)**.** Unsupervised Principal Component Analysis (PCA) and Supervised Partial Least Squares - Discriminant Analysis (PLS-DA) were completed to get a global overview of the metabolic alterations. The variable importance in the projection (VIP) values greater than 1 were considered significant and responsible for group separation [38]. Cluster analysis was performed using Euclidean distance and Ward clustering algorithm of the responsive metabolites detected by PLS-DA VIP score and ANOVA analysis. The changes observed in the normalized abundance of the measured metabolites produced by MetaboAnalyst 5.0 were further displayed in boxplots using GraphPad Prism 9.

The responsive metabolites were further considered in the pathway analyses to identify the most relevant pathways altered [36]. Pathway analysis was performed with MetaboAnalyst 5.0 with respect to the KEGG pathway built-in metabolic library of green alga *Chlorella variabilis* [39]. Pathways with a threshold > 0.1 were considered as significantly dysregulated.

## 3. Results and discussion

### 3.1. Accumulation of Hg(II) and MeHg by Cyclotella meneghiniana

Exposure to Hg(II) and MeHg resulted in a significant increase in THg cellular burden (Fig. 1) compared to the unexposed control treatment, which presented a concentration of (2.18 ± 0.25) × $10^{-5}$ THg pg $cell^{-1}$. Values presented are average ± SD. At the lower exposure concentrations (Hg(II)−1 and MeHg−1), significant differences in cellular THg concentrations ($p < 0.001$) were observed between Hg species treatments, with higher cellular THg in the MeHg−1 exposure. No differences in cellular THg concentrations were found between treatments at the higher concentrations (Hg(II)−2 and MeHg−2). These results are consistent with existing literature for exposure to sub-lethal Hg(II) and MeHg concentrations. For instance, for comparable exposure concentrations in the (sub-)nanomolar range, higher accumulation of MeHg in

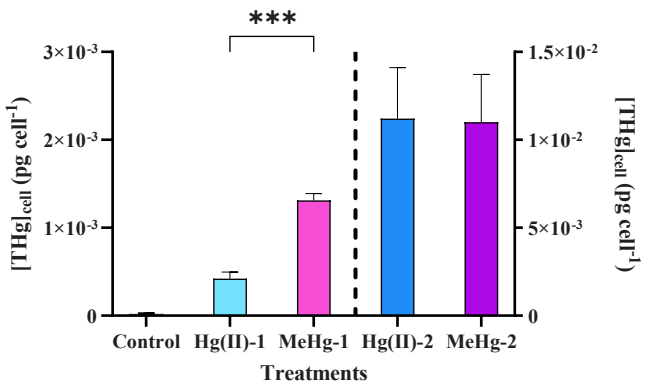


**Fig. 1.** Cellular mercury content ($THg_{cell}$) in *C. meneghiniana* after 2 h-exposure to $8.3 \times 10^{-9}$ M and $6.5 \times 10^{-9}$ M of Hg(II)−1 and MeHg−1; $8.4 \times 10^{-8}$ M and $7.9 \times 10^{-8}$ M of Hg(II)−2 and MeHg−2, respectively. Asterisks indicate significant differences between treatments obtained by a Student's t-test (*** $p < 0.001$).

comparison with Hg(II) was observed in *C. meneghiniana* [40], *C. reinhardtii* [12] and *Synechocystis* sp. [41].

Speciation calculations, as shown in Table S3, indicate that under our experimental conditions, Hg(II) predominantly forms neutral complex, $Hg(OH)_2$, which has been shown to cross cell membranes via passive diffusion [42,43]. MeHg primarily formed positively charged complex, $(CH_3Hg)_2OH^+$, which is likely to penetrate the cell membrane via transporters [44], involving specific transport proteins for metals and AA [12]. At higher exposure concentration, the saturation of the transporters in MeHg exposure [45] could have taken place, whereas the passive diffusion would continue to increase linearly with the Hg(II) exposure concentration, possibly explaining the observed similarity between the cellular concentrations at higher exposure concentration of the two Hg species.

### 3.2. Effect of Hg(II) and MeHg exposure on diatom physiology

Short-term exposure of diatom cells to Hg(II) and MeHg indicated distinct physiological responses. For MeHg treatments, no significant changes were detected after a 2-hour exposure (Fig. 2 **and** Figs. S3-S6) for the following parameters: ROS generation ($3.3 \pm 1.0\%$ and $3.2 \pm 1.4\%$ for MeHg−1 and MeHg−2, respectively), membrane integrity ($17.2 \pm 1.3\%$ and $18.3 \pm 2.5\%$ for MeHg−1 and MeHg−2, respectively), carotenoid concentration ($(4.9 \pm 1.1) \times 10^{-7}$ and $(4.1 \pm 0.5) \times 10^{-7}$ μg $cell^{-1}$ for MeHg−1 and MeHg−2, respectively) and total chlorophyll concentration ($(1.4 \pm 0.3) \times 10^{-6}$ and $(1.3 \pm 0.07) \times 10^{-6}$ μg $cell^{-1}$ for MeHg−1 and MeHg−2, respectively) when compared with the unexposed treatment ($2.9 \pm 1.8\%$ for ROS generation, $16.1 \pm 1.3\%$ for membrane integrity, $(9.7 \pm 2.4) \times 10^{-7}$ and $(4.4 \pm 0.2) \times 10^{-7}$ μg $cell^{-1}$ for total chlorophyll and carotenoids, respectively). Hg(II) exposure resulted in increased cellular ROS generation ($12.1 \pm 4.8\%$ and $13.4 \pm 7.4\%$ for Hg(II)−1 and Hg(II)−2 respectively) with a significant difference for Hg(II)−2 treatment (Fig. 2, Fig. S3). Additionally, chlorophyll autofluorescence was affected in both Hg(II) treatments (Fig. S4), suggesting that the increased ROS production induced by Hg(II) exposure affected diatom photosynthesis. This decrease correlates with the significant decrease in total chlorophyll concentration (Fig. 2) in both Hg(II) treatments ($(6.2 \pm 0.5) \times 10^{-7}$ and $(5.8 \pm 0.3) \times 10^{-7}$ μg $cell^{-1}$ for Hg(II)−1 and Hg(II)−2 respectively), along with a decreasing trend of carotenoid cellular concentration (Fig. S5, $(3.6 \pm 1.4) \times 10^{-7}$ and $(3.4 \pm 0.9) \times 10^{-7}$ μg $cell^{-1}$ for Hg(II)−1 and Hg(II)−2, respectively) compared to the unexposed control. Lastly, the increased ROS production in Hg(II) treatments correlates with the results of membrane integrity (Fig. 2, Fig. S6). Hg(II) treatments displayed an increasing trend in membrane integrity (Hg(II)−1: $22.9 \pm 1.3\%$, $p = 0.1443$ and Hg(II)−2: $23.6 \pm 4.7\%$, $p < 0.05$) in comparison with the control, which is expected since the excess of ROS can induce oxidative damage to lipids (e.g. alteration of the membrane permeability), proteins (e.g. changes in AA) and DNA [46]. Metals, including mercury, have been shown to induce excessive ROS production in algae by damaging photosynthetic systems, impacting iron-mediated processes, or decreasing the antioxidant pool [11,47]. Excessive ROS generation has been observed in phytoplankton species and is believed to depend on exposure concentration and Hg species. For instance, ROS production in *Microcystis aeruginosa* increased after 24 h exposure to concentrations $> 50 \times 10^{-9}$ M but not at concentrations $< 25 \times 10^{-9}$ M Hg(II) [48]. For concentrations between $10^{-10}$ and $10^{-8}$ M of both Hg(II) and MeHg, only the $10^{-10}$ M MeHg treatment resulted in an increased ROS percentage in *C. reinhardtii* cells after a 2 h exposure [12]. This absence of ROS increase was attributed to an efficient antioxidant response at the gene level [12]. The biosynthesis of pigments, fundamental for photosynthesis performance, is known to play a role in the antioxidant defense of algae against metal exposure [49,50]. When exposed to Hg(II) concentrations of 24.9, 49.9 and $99.8 \times 10^{-9}$ M, an increase in the pigment production was observed in the cyanobacterium *M. aeruginosa* [48]. Nevertheless, the inhibition of pigment synthesis and

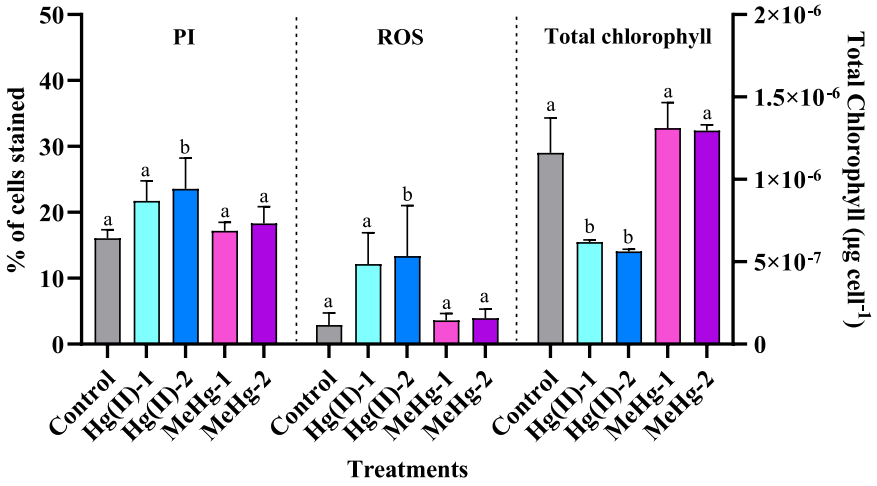


**Fig. 2.** Comparative analysis of the different biological endpoints in diatom cells exposed to Hg(II) (Hg(II)−1 and Hg(II)−2), MeHg (MeHg−1 and MeHg−2), as well as those unexposed to Hg (Control). The left axis describes the percentage of cells with excessive ROS and those with affected membrane integrity; the right axis describes the total chlorophyll content per cell. Letters on the chart indicate significant differences between treatments, as determined by one-way ANOVA followed by a Tukey test ($p < 0.05$).

degradation, presumably due to the substitution of core-cations with Hg (II) and binding to carboxylate groups in chlorophyll, has been recognized as a common effect of Hg(II) exposure [51]. Indeed, total chlorophyll and carotenoid concentrations significantly decreased in green alga *Scenedesmus quadricauda* exposed to micromolar Hg(II) concentrations for 3 days [52]. Notably, the magnitudes of concentrations tested exceed those in our current study. Exposure to $369 \times 10^{-9}$ M of Hg(II) at 4 °C led to a considerable decrease in chlorophyll *a* concentration in marine diatom *Contibriba weissflogii* and dinoflagellate *Amphidinium canterae* [53]. Regarding MeHg exposure, in-vivo chlorophyll *a* measurement after a 2 h exposure of green alga *C. reinhardtii* to MeHg indicated a decrease in the $10 \times 10^{-9}$ M MeHg treatment [12]. However, Protopopov, et al. [54] reported that no significant changes were detected on the pigment apparatus during short-term exposure of *Chlamydomonas moewusiito* to similar concentration used in our study ($10^{-7}$ M MeHg). Considering the data presented, the physiological response of phytoplankton seems dependent on Hg species, its concentration, and the type of algal species. However, it is important to note that the results were obtained under varying exposure conditions, including different Hg concentrations, exposure time, environmental conditions (e.g. temperature), and phytoplankton species, making a direct comparison less straightforward.

As mentioned, no significant differences were found in cellular ROS production, membrane integrity, or pigment concentrations between MeHg treatments and untreated control. This outcome is believed to be due to a more efficient activation of the antioxidant system in *Cyclotella meneghiniana* cells, supported by the metabolomic data, which showed a significant higher concentration of reduced glutathione (GSH) in both MeHg treatments (Fig. 5**B**). Similarly, Beauvais-Fluck, et al. [55] highlighted the capacity of algae to cope with ROS generation through an efficient antioxidant response linked to the gene level. GSH and other sulfur metabolites are important chelators and scavengers of Hg [51], where recently MeHg was shown to bind one glutathione, forming a 1:1 complex GS-MeHg, which was not the case with Hg(II) [41], and thus, aligning with our findings. In summary, our results showed that, in short-term exposure, the physiological response in diatom cells is primarily triggered by Hg(II) and not MeHg.

### 3.3. Metabolic response of *C. meneghiniana* to Hg(II) and MeHg exposure

In the analysis, 82 metabolites were considered, encompassing the major groups of primary metabolites, including AA, antioxidants, FA, nucleobase/side/tide, organic acids/phenolics and sugars/sugar alcohols. Of the 82 analyzed metabolites, 40 were present and quantified in all Hg treatments and the control. To gain a comprehensive understanding of the effects of the different treatments, we conducted an

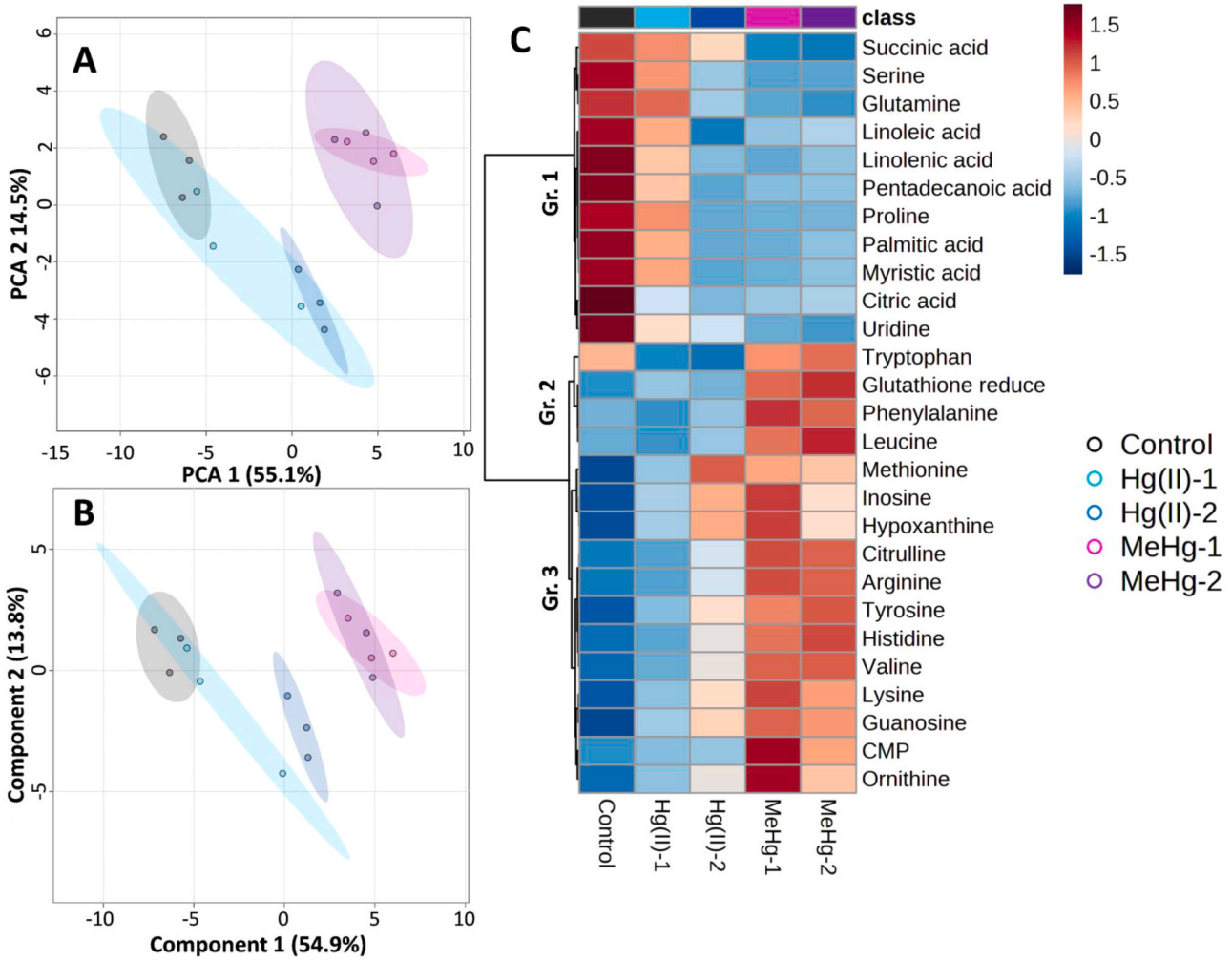


**Fig. 3.** (A) Principal component analysis (PCA) and (B) partial least-squares discriminate analysis (PLS-DA) score plots of the metabolic profiles in *Cyclotella meneghiniana* exposed to $8.3 \times 10^{-9}$ M and $8.4 \times 10^{-8}$ M of Hg(II) for Hg(II)−1 and Hg(II)−2 as well as $6.5 \times 10^{-9}$ M and $7.9 \times 10^{-8}$ M of MeHg for MeHg−1 and MeHg−2, with untreated control ($5.1 \times 10^{-11}$ M THg). (C) Heatmap of the responsive metabolites. Metabolites and samples are clustered hierarchically for better visualization using Euclidian distance measure and Ward cluster algorithm based on the normalized data. The PCA, PLS-DA score plots and heatmap were generated using MetaboAnalyst 5.0 (https://www.metaboanalyst.ca/).

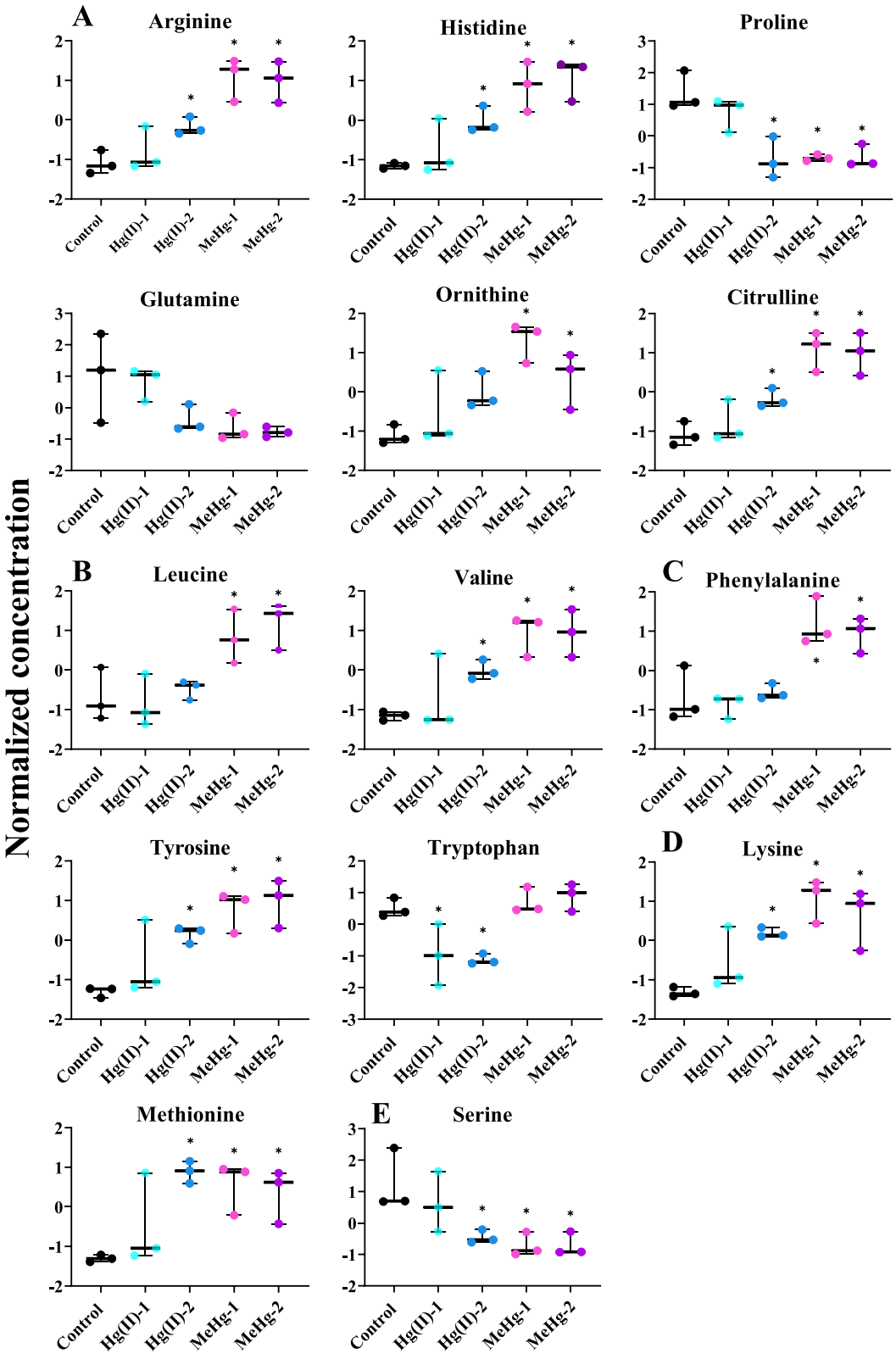


**Fig. 4.** Box plots of the normalized relative abundance of amino acids with significant alterations were obtained in the ANOVA and PLS-DA VIP scores analysis. **(A)** α-ketoglutarate-derived amino acids: arginine, histidine, proline, glutamine, ornithine and citrulline; **(B)** Pyruvate – derived amino acid: leucine and valine; **(C)** Phosphoenolpyruvate derived amino acids: phenylalanine, tyrosine and tryptophan; **(D)** Oxaloacetic acid derived amino acids: lysine and methionine; **(E)** Photo-respiratory glycolate pathway: serine. Five treatments exposed to $8.3 \times 10^{-9}$ M and $8.4 \times 10^{-8}$ M of Hg(II) for Hg(II)– 1 and Hg(II)– 2 as well as $6.5 \times 10^{-9}$ M and $7.9 \times 10^{-8}$ M of MeHg for MeHg-1 and MeHg-2, with untreated controls included. All conditions were performed in triplicate. Asterisks (*) indicate significant differences ($p < 0.05$) between treatments and controls determined by ANOVA analysis.

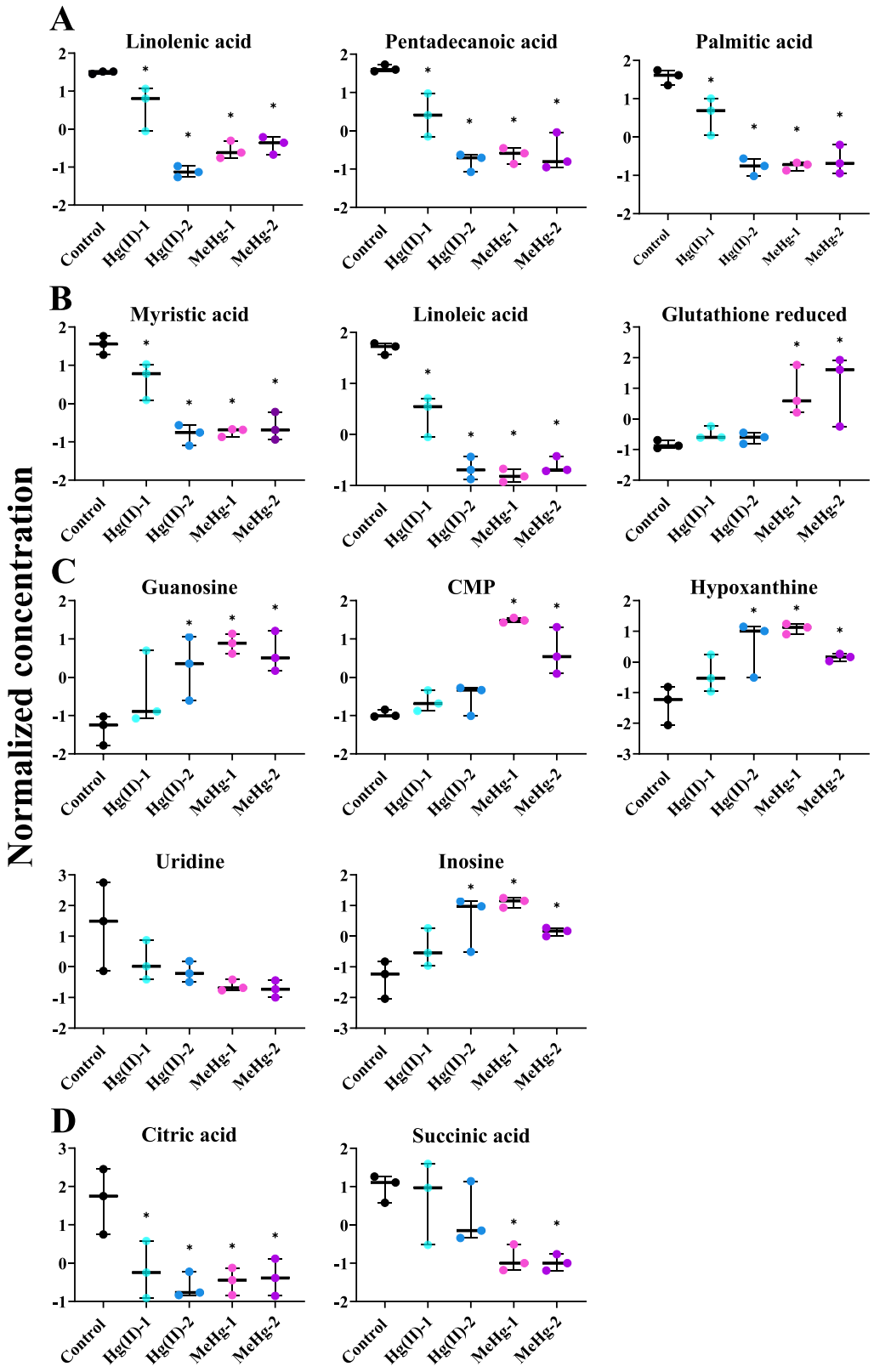


**Fig. 5.** Box plots of the normalized relative abundance concentrations of fatty acids, organic acids, antioxidants and amino acids. **(A)** unsaturated and saturated fatty acids: linolenic acid, myristic acid, linoleic acid, pentadecanoic acid and palmitic acid; **(B)** antioxidants: glutathione reduced; **(C)** nucleobase/side/tide: guanosine, cytidine monophosphate (CMP), hypoxanthine, uridine and inosine; **(D)** organic acids: citric acid and succinic acid. Five treatments exposed to $8.3 \times 10^{-9}$ M and $8.4 \times 10^{-8}$ M of Hg(II) for Hg(II)−1 and Hg(II)−2 as well as $6.5 \times 10^{-9}$ M and $7.9 \times 10^{-8}$ M of MeHg for MeHg−1 and MeHg−2, with untreated controls included. All conditions were performed in triplicate. Asterisks (*) indicate significant differences ($p < 0.05$) between treatments and control, as determined by ANOVA analysis.

unsupervised principal component analysis (PCA), a supervised partial least squares discriminant analysis (PLS-DA), and a clustering analysis (Fig. 3).

The PCA score plot (Fig. 3**A**) demonstrates the separation of MeHg treatments from the control along the first principal component (PC1), which explains 55.1% of the total variance. However, the different Hg (II) and control treatments do not differentiate clearly. In contrast, the PLS-DA presented a clearer separation between MeHg and Hg(II)−2 treatments and the control group (Fig. 3**B**). Nonetheless, there is no separation between Hg(II)−1 treatment and the control group. From the PLS-DA VIP score analysis (VIP> 1; Fig. S7) and the multivariate analysis (ANOVA, $p < 0.05$, Table S6), 27 metabolites showed significant changes in their levels (hereafter responsive metabolites).

The heatmap clustering of the responsive metabolites (Fig. 3**C**) revealed the presence of three major groups. *Group 1* consisted of 11 metabolites (5 FA, 3 AA, 2 carboxylic acids and 1 nucleotide). These metabolites presented reduced concentration levels in response to both Hg(II) and MeHg treatments compared to the control. The depletion was more pronounced in MeHg treatments, emphasizing the importance of Hg speciation. The decrease followed a concentration-dependence response for Hg(II) exposures. *Groups 2* and *3* included 16 metabolites, whose levels increased compared to the control. Group 2 was comprised of four metabolites (3 AA and 1 antioxidant). Noteworthy, significant changes were only observed in MeHg treatments, resulting in a general increase in metabolite concentrations. With the exception of tryptophan, Hg(II) treatments showed no significant variations. Group 3 included 12 metabolites (8 AA and 4 nucleotides) and displayed a significant metabolite accumulation when exposed to MeHg treatments. Hg(II) exposure also triggered an accumulation of these metabolites, which was more evident at higher concentrations (Hg(II)−2), indicating a concentration-dependent response.

In general, the observed alterations in the responsive metabolites were more pronounced under MeHg treatments. While no clear distinction exists between MeHg exposure concentrations, a concentration-dependent response was observed for Hg(II) treatments.

The observed differences can be attributed to the distinct binding preferences of the two mercury forms. Hg(II) is known to primarily bind to cellular structures, including the cell wall, membrane, and other cellular debris. In contrast, MeHg permeates the membrane to accumulate predominantly within the cytoplasm [10]. This MeHg transport mechanism is evidenced by studies highlighting its active transport by microalgae [56,57]. As extracellular Hg(II) concentrations increase, the binding sites in the cellular debris likely become saturated. When this saturation occurs, Hg(II) starts to accumulate more significantly in other cellular compartments [10,42]. This mechanism potentially explains the concentration-dependent results observed for Hg(II) treatments and the comparable results observed in MeHg treatments.

### 3.4. Pathway analysis of *Cyclotella meneghiniana* exposed to Hg(II) and MeHg

A pathway analysis on the responsive metabolites was performed to identify the biological pathways potentially undergoing significant dysregulation due to mercury exposure. The combined analysis of Hg(II) and MeHg treatments revealed 12 significantly impacted pathways (Fig. S8, Table S7). The impacted pathways (threshold > 0.1) included linoleic acid metabolism, isoquinoline alkaloid biosynthesis, phenylalanine metabolism, tyrosine metabolism, glutathione metabolism, arginine biosynthesis, alanine, aspartate and glutamate metabolism, arginine and proline metabolism, tryptophan metabolism, cysteine and methionine metabolism, alpha-linolenic acid metabolism, and citrate cycle (also known as tricarboxylic acid cycle – TCA cycle). These results highlight the sensitivity of diatom *Cyclotella meneghiniana* toward exposure to Hg species. Six of these pathways, such as alpha-linolenic acid metabolism, alanine, aspartate and glutamate metabolism, arginine and proline metabolism, arginine biosynthesis, glutathione metabolism and isoquinoline alkaloid biosynthesis, were common with those observed in green alga *C. reinhardtii* exposed to Hg(II) or MeHg [22]. Interestingly, the alpha-linolenic acid metabolism was significantly disturbed by both Hg(II) and MeHg exposure in *C. meneghiniana*, while in *C. reinhardtii* only by Hg(II), with MeHg having no apparent impact [22]. Similar metabolic pathways were affected after exposing *E. gracilis* to Hg(II), including the glutathione metabolism and TCA cycle [21]. The increased number of disrupted metabolic pathways in *Cyclotella meneghiniana*, when compared to other species under similar exposures (e.g. *C. reinhardtii*) and higher exposures (e.g. $5.0 \times 10^{-6}$ M of Hg(II) in *E. gracilis*), evidences the elavated sensitivity of diatoms towards pollutants [58].

### 3.5. Metabolic perturbation in *Cyclotella meneghiniana* exposed to Hg(II) and MeHg

The metabolites exhibiting dysregulated responses were similar for both Hg(II) and MeHg. They included 14 amino acids, 1 antioxidant, 5 fatty acids, 2 carboxylic acids, and 5 nucleobase/side/tides. However, the response intensity differed between Hg(II) and MeHg treatments.

**Amino acids metabolism:** A significant decrease ($p < 0.05$) in the relative abundance of 14 AA (arginine, histidine, proline, glutamine, ornithine, citrulline, leucine, valine, phenylalanine, tyrosine, tryptophan, lysine, methionine and serine) out of 21 measured was observed after 2 h exposure to Hg(II) and MeHg treatments (Fig. 4). This suggests that Hg exposure induced a significant alteration of the amino acid synthesis [59] and/or potential degradation of proteins and polypeptides, and other related biological processes [60], where AA serve as precursors for the synthesis of various metabolites and nucleotides.

In fact, arginine, citrulline, histidine and ornithine, which derive from the TCA metabolite α-ketoglutarate [61], increased significantly in the diatom cells treated with Hg(II) and MeHg (Fig. 4**A**). The increase in the concentration of these metabolites was more pronounced for MeHg treatments and for the Hg(II)−2 treatment. As ornithine, citrulline, and arginine are part of the urea cycle in diatoms, the results also suggest an acceleration of the urea cycle, which in diatoms serves in the reallocation of intracellular carbon (C) and nitrogen (N); and the formation of carbonaceous and nitrogenous compounds necessary for growth [62]. In addition, the ornithine-urea cycle in diatoms is closely linked to the TCA cycle [63]; hence, exposure to MeHg and Hg(II) alters the fixation of both C and N.

As histidine is necessary for the normal growth and development of algal cells [64,65], its accumulation suggests a potential impact of Hg(II) and, particularly, MeHg treatments on the growth and development of diatom cells. In addition, histidine and arginine play roles in deamination processes in plant cells [66].

The concentrations of glutamine and proline decreased in both MeHg treatments and Hg(II)−2 (Fig. 4**A**), though the effect was more pronounced in MeHg treatments. The significant depletion of proline can be considered a possible response against Hg stress since it plays an essential role in osmo- and redox-regulation, metal chelation, and scavenging of free radicals induced by different metals in plants [67,68]. This finding contrasts with the increase of glutamine and proline abundance observed upon exposure to Hg(II) and MeHg in *C. reinhardtii* [22] and an increase in proline in *E. gracilis* [21]. Such differences in response to Hg species suggest a species-specific response.

The concentrations of leucine and valine, produced from pyruvate [60], significantly increased ($p < 0.05$) in cells treated with Hg (Fig. 4**B**). The accumulation was more prominent in MeHg treatments and increased with the exposure concentrations for leucine, but not for valine. A similar increase in the abundance of leucine and valine was observed in green alga *C. reinhardtii* for comparable concentrations of Hg (II) or MeHg [22], as well as in valine abundance in *E. gracilis* [21]. Leucine serves as an oxidative phosphorylation energy source in plant cells [69]. Leucine and valine can be converted to acetyl-CoA and presumably be used as a substrate for the TCA cycle or contribute to

triacylglycerol metabolism by providing carbon precursors and ATP as previously shown for green alga *C. reinhardtii* [70]. Indeed, leucine and valine and their degradation products have been shown to include acetyl-CoA, which serves as potential substrate for de novo fatty acid synthesis [71]. Hence, the accumulation of these metabolites in *Cyclotella meneghiniana* cells may indicate a response to the increasing need for energy to cope with Hg(II) and MeHg stress.

Phenylalanine abundances increased significantly only in response to MeHg treatments (Fig. 4**C**), while tyrosine, a precursor of various structurally diverse compounds [72], accumulated in both treatments. Compared to the control, the accumulation of tyrosine abundance increased with higher Hg(II) concentrations, showing a concentration-dependence, with no difference between MeHg and Hg (II) treatments despite an overall higher accumulation of tyrosine. Notably, these AA accumulated in *C. reinhardtii* when exposed to either Hg(II) or MeHg [22]. Both of these AA are precursors for the synthesis of pigments, including carotenoids and phytochelatins [73], which play a protective role for the photosynthetic apparatus of algae against oxidative damage [74]. Hence, the accumulation of AA could lead to the acceleration of the biosynthesis of carotenoids and the enhancement of cellular defense mechanisms. However, no significant changes were detected in carotenoid concentration between treatments and control (Fig. S3). These findings can be interpreted in different ways, for example, (i) the increase of the metabolites is not the end product being dependent on other components (e.g. enzymes), (ii) the increased metabolites can be used on alternative pathways, and (iii) the increase of production of pigments is counterbalanced by their degradation (induced by MeHg exposure), leading to no discernible net change.

Among the AA derived from aspartate, both lysine and methionine concentrations were significantly augmented in the cells treated with Hg (II) and MeHg (Fig. 4**D**). The observed alterations were concentration-dependent for Hg(II) exposure. In contrast, no significant differences were observed between the MeHg treatments. As methionine can be used as a surrogate for the estimation of the rate of protein synthesis [75], the results imply a significant acceleration in protein synthesis rates. Additionally, methionine contains SH- groups and, similarly to glutathione (GSH), can act as a chelator and scavenger of mercury [76], thus being involved in the sequestration and detoxification of Hg species in the diatom.

The concentration of serine in diatom cells exposed to Hg(II) and MeHg decreased significantly (Fig. 4**E**). This reduction was significant for both MeHg treatments and Hg(II)−2. Meanwhile, glycine concentrations remained unchanged across the different treatments. These two AA are synthesized during the photorespiratory glycolate cycle [60,77], and the Gly/Ser ratio is often employed as a measure of photorespiratory activity [78]. The Gly/Ser ratio increased from $2.72 \pm 0.29$ for the control to $6.83 \pm 1.80$ and $6.13 \pm 1.14$ for MeHg−1 and MeHg−2, respectively. In the Hg(II) treatments, it ranged from $3.29 \pm 0.64$ and $3.75 \pm 0.99$ for Hg(II)−1 and Hg(II)−2, respectively. These results demonstrate that Hg(II) and, in particular MeHg, induce significant upregulation in photorespiration. This upregulation likely provides additional energy for synthesizing various defense components to cope with oxidative stress. For instance, photorespiration can also provide protection against oxidative damage by supplying glycine to synthesize the antioxidant glutathione [78,79], an upregulated process in our study (further discussed in the *Antioxidant metabolism section*). Furthermore, photorespiration can act as an "energy sink", preventing the over-reduction of the photosynthetic electron transport chain and photoinhibition, especially under stress conditions [79]. These findings are consistent with a previous study where photorespiration activity was accelerated in *P. malhamensis* upon exposure to $AgNO_3$ and Ag nanoparticles [19]. Furthermore, glycine and serine levels exhibited significant increases in *C. reinhardtii* after exposure to Hg(II) and MeHg. This increase was likewise interpreted as an acceleration of the photorespiratory activity to cope with Hg stress, though no Gly/Ser ratio changes were observed [22].

The findings from the current study are consistent with previous studies that have shown significant alterations in amino acid metabolism in different phytoplankton species when exposed to different contaminants. For example, green alga *Chlorella* sp. [17,80], *Scenedesmus quadricauda* [15] and diatom *Tabellaria flocculosa* [16] exposed to $Cu^{2+}$, *P. malhamensis* exposed to AgNPs and $Ag^{+}$ [19], *C. reinhardtii* exposed to $nTiO_2$ [20], and to Hg(II) and MeHg [22], and *E. gracilis* exposed to Hg(II) [21].

**Fatty acids metabolism:** The abundances of three saturated acids, i.e. myristic acid (tetradecanoic acid, 14:0), pentadecylic acid (pentadecanoic acid, 15:0) and palmitic acid (hexadecanoic acid, 16:0), and two unsaturated acids, i.e. linolenic acid (C 9,12,15 double bonds) and linoleic acid (C 9,12 double bonds) decreased significantly in the diatom cells exposed to Hg(II) and MeHg, with a concentration-dependent response in the case of Hg(II) (Fig. 5**A**). Our findings indicate significant unsaturation of the lipid membranes and possible alteration of their permeability and integrity. However, membrane integrity was only significantly affected in the Hg(II)−2 treatment, while the percentage of the cells with affected membranes in the MeHg treatments was comparable to the control group (Fig. 2**B**). Diatoms are known for their ability to accumulate large amounts energy-rich lipids. Therefore, the oxidation of these lipids offers an alternative way for cells to generate energy [16]. This suggests that the decline in fatty acid abundance is suggestive of the degradation of the stored FA into acetyl-CoA. Consequently, this can be used in the TCA cycle to generate energy [81], likely an alternative way to cope with the stress response.

Our results are in general agreement with the decrease in concentrations of fatty acids in *E. gracilis* exposed to Hg(II) [21], the decrease in the saturated FA in *P. malhamensis* treated with AgNPs [19]; reduction of monounsaturated and polyunsaturated FA in *C. vulgaris* exposed to AgNPs and $Ag^{+}$ [82]. However, an accumulation of linolenic, linoleic and palmitic acids was found in *C. reinhardii* exposed to Hg(II) [22].

**Antioxidant metabolism:** Among the 8 antioxidant metabolites considered, only the abundance of glutathione reduced was significantly increased in the two MeHg treatments (Fig. 5**B**). Reduced GSH concentration in Hg(II) treatments was comparable with the control group. As GSH plays a central role in cellular redox regulation [83], the increase in its concentration upon MeHg exposure suggests the activation of a defense mechanism against oxidative stress induced by mercury exposure. This defense appears to be Hg species-specific, being triggered by MeHg, but not Hg(II). This assumption is further supported by a clear increase in ROS percentage in Hg(II) treatments, a response not observed in MeHg treatments (Fig. 2**A**). Furthermore, reduced GSH is a precursor of the synthesis of phytochelatins (-Glu-Cys)n-Gly with n = 2–11, PCn), which can be activated by different toxic metals, including Hg, and is considered a major intracellular chelator for Hg detoxification [11,84]. However, the low capacity of diatom cells to induce PCn production in the presence of MeHg was previously highlighted [85]. The importance of GSH as the main low molecular weight binding ligand to Hg(II) ((GS)2-Hg) and MeHg (GS-MeHg) in the cytosol of cyanobacterium *Synechocystis* sp. PCC 6803 has been recently demonstrated [41]. The GS-MeHg complex (methylmercury-S-glutathione) may also form in diatoms, but further research is necessary to confirm this hypothesis.

An increase in reduced GSH concentration is a common defense mechanism observed in different phytoplankton species exposed to different pollutants. For example, an increase in reduced GSH was observed in the green alga *C reinhardtii* exposed to both Hg(II) and MeHg [22], green alga *E. gracilis* exposed to Hg(II) [21], and *P. melhamensis* exposed to AgNP and dissolved Ag [19]. However, Hg(II) exposure significantly decreased the GSH cellular concentrations in other green algae, *Cosmarium conspersum* and *C. autotrophica* [86].

**Nucleobase/tide/side metabolism:** Out of the 7 nucleobase/tide/sides detected, 5 were significantly different between Hg(II) and MeHg treatments, and the control ($p < 0.05$) (Fig. 5**C**). Pyrimidine nucleotide cytidine monophosphate (CMP) significantly accumulated in both MeHg

treatments but not in Hg(II) treatments. Uridine levels decreased in all treatments, suggesting reduced RNA synthesis or increased RNA degradation. The purine metabolites guanosine, hypoxanthine and inosine significantly increased in Hg(II) and MeHg treatments, with Hg (II) indicating a concentration-dependent response. Guanosine and hypoxanthine metabolites increased after exposing *C. reinhardtii* to Hg(II) and MeHg [22]. Purine pathway was identified as one of the affected pathways after exposing *E. gracilis* to Hg(II) [21]. Therefore, the accumulation of some pyrimidine and purine metabolites suggests the increase of their biosynthesis or the upregulation of the salvage pathway, where existing DNA and RNA molecules are recycled into mononucleotides [87]. To a certain extent, our assumptions align with the increased abundance of AA, considering that AA can act as precursors for various metabolites, including purine and pyrimidine nucleotides [60].

**Carboxylic acid metabolism:** Out of the 4 organic acids detected, two were significantly dysregulated in all treatments (Fig. 5**D**). Citric and succinic acids, key TCA cycle metabolites, displayed significant decreases in all treatments, except for succinic acid in the Hg(II)−1 treatment. It is important to point out that the TCA cycle serves as the central core of the cellular respiratory machinery. Hence, the observed decrease in TCA intermediates could likely be related to their consumption to produce the energy required for manufacturing defense compounds needed to cope with the stress induced by Hg. A similar decrease in the TCA intermediates was observed in the diatom *Tabellaria flocculosa* exposed to high Cu concentrations [16]. The observed differences appear to be species-specific, as metabolomic results from other algae exposed to various pollutants revealed opposite trends. For example, exposure to Hg(II) and MeHg of the green alga *C. reinhardtii* increased the abundance of succinic acid, malic acid and citric acid [22]. Succinic acid concentrations increased significantly in *P. malhamensis* [19], and *C. vulgaris* [18] exposed to $Ag^{+}$ and AgNPs, and in *C. reinhardtii* exposed to increasing concentrations of $nTiO_2$ [20].

Using the significantly altered metabolites, a conceptual scheme illustrating the impact of high concentrations of Hg(II) and MeHg, representative for contaminated environment on the metabolism of diatom *C. meneghiniana* is provided in Fig. 6. The results have important environmental implications for given the vital role of diatoms in C and N- fixation and Si turnover in aquatic environment. Furthermore, the lipid and fatty acid abundances significantly reduced across all treatments. This indicates that in environments with high contamination, not only diatoms physiology is compromised, but their nutritional value for predators is also reduced. Such changes can have eological and functional consequences. In fact, given that diatoms have a high lipid and fatty acid content [88,89], they serve as a particularly valuable food source for a variety of aquatic organisms [89,90]. The decline in their lipid content could have an impact in the aquatic food web.

The remaining metabolites presented a perturbation in all treatments or at least one of each Hg species. Pathways networks are simplified, and metabolites can be generated from other direct or indirect pathways apart from the ones presented. Abbreviations: PPRP: 5-Phosphoribosyl 1-pyrophosphate, dTMP: Deoxythymidine 5′-phosphate, UMP: Uridine 5′-monophosphate, CMP: Cytidine-5′-monophosphate, GMP: Guanosine 5′-monophosphate, XMP: Xanthosine 5′-phosphate, IMP: Inosine 5′-monophosphate. The pathway scheme was based on KEGG database resource platform.

## 4. Conclusions

The present study has, for the first time, studies the metabolomic perturbations induced by Hg(II) and MeHg following their accumulation in the diatom *C. meneghiniana* during short-term exposure under conditions representative of contaminated environments. The results highlight that both Hg species cause significant metabolic perturbations in diatom cells, affecting amino acids, nucleotides, fatty acids, TCA, and antioxidant metabolism. The metabolic shifts, while discernible across multiple pathways for both Hg species, exhibited distinct trends. The exposure to Hg(II) led to a concentration-dependent impact on the metabolism and had a tangible physiological influence, as evidenced by increased ROS generation, compromised membrane integrity, and

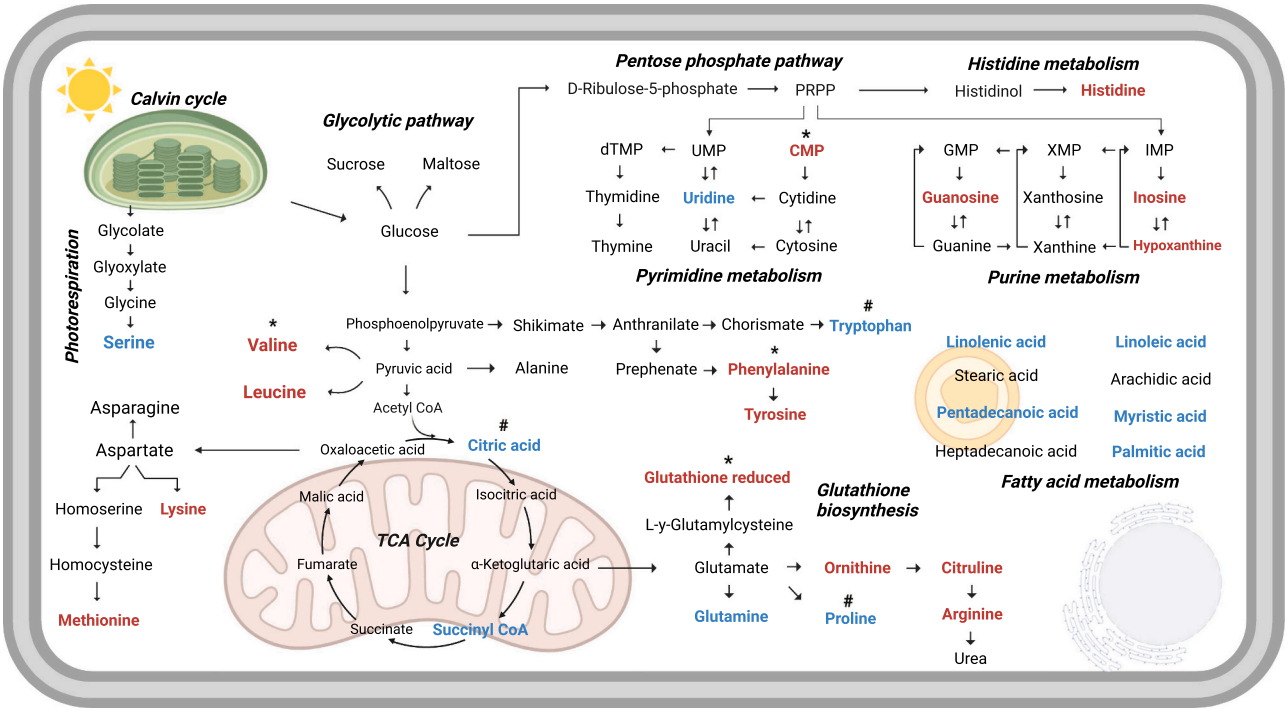


**Fig. 6.** Summary of the overall perturbations induced by Hg(II) and MeHg exposure in diatom *Cyclotella meneghiniana.* Depleted metabolites are presented in blue, and accumulated metabolites are in red. The asterisk (*) indicates perturbations observed only in MeHg treatments, while the cardinal (#) symbol indicates perturbations only seen in Hg(II) treatments.

reduced chlorophyll concentration. The exposure to MeHg induced a more intense reprogramming of the diatoms' metabolism to counter its harmful effect. This pronounced response is characterized by increased energy production and a robust antioxidant defense, maintaining the levels of physiological endpoints.

Elevated Hg concentrations can impact ecosystem dynamics, as they lead to increased photorespiration and consequently, a reduction in carbon fixation, as well as a decline in lipid and carbohydrate levels, potentially disturbing the global carbon cycle.

The outcomes of this study demonstrated the importance of metabolomic analysis to assess and understand the different yet subtle cellular response changes in phytoplankton species exposed to different concentrations and speciation of mercury.

## Environmental implication

Mercury is a hazardous pollutant of global importance. Despite their pivotal role in biogeochemical cycles, a significant knowledge gap exists regarding the metabolic perturbations induced by mercury in phytoplankton. The study explores the metabolic alterations in freshwater diatom induced by sub-lethal inorganic and methyl mercury concentrations, major aquatic mercury species. The results highlighted that diatom reprograms the metabolism of amino acids, nucleotides, fatty acids, carboxylic acids and antioxidants to cope with Hg-induced stress in a mercury-species dependent manner. The results have important environmental implications for contaminated environment given the vital role of diatoms in C and N- fixation and Si turnover.

## Author contributions

V.I.S., and J.P.S. conceived and designed the study. J.P.S. performed the bioassays for bioaccumulation, physiological response assessment, exposure assays for metabolomics, analyzed the physiological response data and provided interpretation and wrote this part of the manuscript; W. L. performed the LC–MS measurements and data processing, V.I.S. and J.P.S. performed treatment and interpretation of metabolomics results, V.I.S. wrote the metabolomics part of the manuscript, overviewed the overall study. A.A.K. took part in the data interpretation, manuscript writing, overviewed the overall study. All the authors critically commented and revised the manuscript. All the authors have approved the paper submission.

## CRediT authorship contribution statement

**Slaveykova Vera I.:** Conceptualization, Formal analysis, Funding acquisition, Methodology, Resources, Supervision, Validation, Writing – review & editing, Writing – original draft. **Li Weiwei:** Investigation, Writing – review & editing. **Keller Arturo A.:** Conceptualization, Validation, Writing – review & editing. **Santos João Pereira:** Conceptualization, Data curation, Formal analysis, Investigation, Methodology, Validation, Visualization, Writing – original draft, Writing – review & editing.

## Declaration of Competing Interest

The authors declare that they have no known competing financial interests or personal relationships that could have appeared to influence the work reported in this paper.

## Data Availability

Data will be made available on request.

## Acknowledgements

The present study was financially supported by the Swiss National Science Foundation grants 180186 and 175721. Any opinions, findings, conclusions or recommendations expressed in this material are those of the author(s) and do not necessarily reflect the views of the funding agencies.

## Appendix A. Supporting information

Supplementary data associated with this article can be found in the online version at doi:10.1016/j.jhazmat.2023.133245.

## References

[1] Branfireun, B.A., Cosio, C., Poulain, A.J., Riise, G., Bravo, A.G., 2020. Mercury cycling in freshwater systems - An updated conceptual model. Sci Total Environ 745, 140906. https://doi.org/10.1016/j.scitotenv.2020.140906.
[2] Zhu, S., Zhang, Z., Zagar, D., 2018. Mercury transport and fate models in aquatic systems: a review and synthesis. Sci Total Environ 639, 538–549. https://doi.org/10.1016/j.scitotenv.2018.04.397.
[3] Ariya, P.A., Amyot, M., Dastoor, A., Deeds, D., Feinberg, A., Kos, G., et al., 2015. Mercury physicochemical and biogeochemical transformation in the atmosphere and at atmospheric interfaces: a review and future directions. Chem Rev 115 (10), 3760–3802. https://doi.org/10.1021/cr500667e.
[4] Riaz, A., Khan, S., Muhammad, S., Shah, M.T., 2019. Mercury contamination in water and sediments and the associated health risk: a case study of artisanal gold-mining. Mine Water Environ 38 (4), 847–854. https://doi.org/10.1007/s10230-019-00613-5.
[5] Forti, V., Balde, C.P., Kuehr, R. & Bel, G., 2020. The Global E-waste Monitor 2020: Quantities, flows and the circular economy potential.
[6] Aubrac, G., Bastiansz, A., Basu, N., 2022. Systematic review and meta-analysis of mercury exposure among populations and environments in contact with electronic waste. Int J Environ Res Public Health 19 (19). https://doi.org/10.3390/ijerph191911843.
[7] Lavoie, R.A., Jardine, T.D., Chumchal, M.M., Kidd, K.A., Campbell, L.M., 2013. Biomagnification of mercury in aquatic food webs: a worldwide meta-analysis. Environ Sci Technol 47 (23), 13385–13394. https://doi.org/10.1021/es403103t.
[8] Cordoba-Tovar, L., Marrugo-Negrete, J., Baron, P.R., Diez, S., 2022. Drivers of biomagnification of Hg, As and Se in aquatic food webs: a review. Environ Res 204 (Pt C), 112226. https://doi.org/10.1016/j.envres.2021.112226.
[9] Tada, Y., Marumoto, K., 2020. Uptake of methylmercury by marine microalgae and its bioaccumulation in them. J Oceanogr 76 (1), 63–70. https://doi.org/10.1007/s10872-019-00525-6.
[10] Wu, Y., Wang, W.X., 2011. Accumulation, subcellular distribution and toxicity of inorganic mercury and methylmercury in marine phytoplankton. Environ Pollut 159 (10), 3097–3105. https://doi.org/10.1016/j.envpol.2011.04.012.
[11] Le Faucheur, S., Campbell, P.G., Fortin, C., Slaveykova, V.I., 2014. Interactions between mercury and phytoplankton: speciation, bioavailability, and internal handling. Environ Toxicol Chem 33 (6), 1211–1224. https://doi.org/10.1002/etc.2424.
[12] Beauvais-Fluck, R., Slaveykova, V.I., Cosio, C., 2017. Cellular toxicity pathways of inorganic and methyl mercury in the green microalga *Chlamydomonas reinhardtii*. Sci Rep 7 (1), 8034. https://doi.org/10.1038/s41598-017-08515-8.
[13] Dumas, T., Courant, F., Fenet, H., Gomez, E., 2022. Environmental metabolomics promises and achievements in the field of aquatic ecotoxicology: viewed through the pharmaceutical lens. Metabolites 12 (2). https://doi.org/10.3390/metabo12020186.
[14] Wei, S., Wei, Y., Gong, Y., Chen, Y., Cui, J., Li, L., et al., 2022. Metabolomics as a valid analytical technique in environmental exposure research: application and progress. Metabolomics 18 (6), 35. https://doi.org/10.1007/s11306-022-01895-7.
[15] Yong, W.K., Sim, K.S., Poong, S.W., Wei, D., Phang, S.M., Lim, P.E., 2018. Interactive effects of temperature and copper toxicity on photosynthetic efficiency and metabolic plasticity in (*Chlorophyceae*). J Appl Phycol 30 (6), 3029–3041. https://doi.org/10.1007/s10811-018-1574-3.
[16] Goncalves, S., Kahlert, M., Almeida, S.F.P., Figueira, E., 2018. Assessing Cu impacts on freshwater diatoms: biochemical and metabolomic responses of *Tabellaria flocculosa* (Roth) Kutzing. Sci Total Environ 625, 1234–1246. https://doi.org/10.1016/j.scitotenv.2017.12.320.
[17] Zhang, W., Tan, N.G., Fu, B., Li, S.F., 2015. Metallomics and NMR-based metabolomics of *Chlorella* sp. reveal the synergistic role of copper and cadmium in multi-metal toxicity and oxidative stress. Metallomics 7 (3), 426–438. https://doi.org/10.1039/c4mt00253a.
[18] Qu, R., Xie, Q., Tian, J., Zhou, M., Ge, F., 2021. Metabolomics reveals the inhibition on phosphorus assimilation in *Chlorella vulgaris* F1068 exposed to AgNPs. Sci Total Environ 770, 145362. https://doi.org/10.1016/j.scitotenv.2021.145362.
[19] Liu, W., Majumdar, S., Li, W., Keller, A.A., Slaveykova, V.I., 2020. Metabolomics for early detection of stress in freshwater alga *Poteriochromonas malhamensis* exposed to silver nanoparticles. Sci Rep 10 (1), 20563. https://doi.org/10.1038/s41598-020-77521-0.
[20] Liu, W., Li, M., Li, W., Keller, A.A., Slaveykova, V.I., 2022. Metabolic alterations in alga *Chlamydomonas reinhardtii* exposed to nTiO(2) materials. Environ Sci Nano 9 (8), 2922–2938. https://doi.org/10.1039/d2en00260d.

[21] Mangal, V., Donaldson, M.E., Lewis, A., Saville, B.J., Guéguen, C., 2022. Identifying metabolic and transcriptomic adaptations in response to mercury stress. Front Environ Sci 10. https://doi.org/10.3389/fenvs.2022.836732.

[22] Slaveykova, V.I., Majumdar, S., Regier, N., Li, W., Keller, A.A., 2021. Metabolomic responses of green Alga *Chlamydomonas reinhardtii* exposed to sublethal concentrations of inorganic and methylmercury. Environ Sci Technol 55 (6), 3876–3887. https://doi.org/10.1021/acs.est.0c08416.

[23] Serôdio, J., Lavaud, J., 2022. Diatoms and their ecological importance. Life Below Water. Springer, pp. 304–312.

[24] Ragueneau, O., Schultes, S., Bidle, K., Claquin, P., Moriceau, B., 2006. Si and C interactions in the world ocean: Importance of ecological processes and implications for the role of diatoms in the biological pump. Glob Biogeochem Cycles 20 (4). https://doi.org/10.1029/2006gb002688.

[25] Davis, A., Abbriano, R., Smith, S.R., Hildebrand, M., 2017. Clarification of photorespiratory processes and the role of malic enzyme in diatoms. Protist 168 (1), 134–153. https://doi.org/10.1016/j.protis.2016.10.005.

[26] Seckbach, J., Kociolek, P., 2011. The diatom world. Springer Science & Business Media.

[27] Kelly, M., Bennett, C., Coste, M., Delgado, C., Delmas, F., Denys, L., et al., 2008. A comparison of national approaches to setting ecological status boundaries in phytobenthos assessment for the European Water Framework Directive: results of an intercalibration exercise. Hydrobiologia 621 (1), 169–182. https://doi.org/10.1007/s10750-008-9641-4.

[28] Metcalf, A.J., Boyle, N.R., 2022. Rhythm of the night (and Day): predictive metabolic modeling of diurnal growth in *Chlamydomonas*. mSystems 7 (4), e0017622. https://doi.org/10.1128/msystems.00176-22.

[29] Caballero-Gallardo, K., Palomares-Bolaños, J., Olivero-Verbel, J., 2022. Mercury concentrations in water, sediments, soil, and fish around ancestral afro-descendant territories impacted by gold mining in the cauca department, Colombia. Water Air Soil Poll 233 (9). https://doi.org/10.1007/s11270-022-05779-3.

[30] Santos, J.P., 2023, September. The Role of *Cyclotella meneghiniana* in Mercury Cycling: Evidence of CH3Hg Demethylation and Hg(II) Reduction [Conference presentation, No. 92571] First Joint ICOBTE-ICHMET 2023. University of Wuppertal, Germany.

[31] Santos, J.P., Mehmeti, L., Slaveykova, V.I., 2022. Simple acid digestion procedure for the determination of total mercury in plankton by cold vapor atomic fluorescence spectroscopy. Methods Protoc 5 (2), 29. https://doi.org/10.3390/mps5020029.

[32] Environmental Protection Agency, U. S. Method 1631, Revision E: Mercury in Water by Oxidation, Purge and Trap, and Cold Vapor Atomic Fluorescence Spectrometry. 36 p. (Office of Water, 2002).

[33] Osório, C, Machado, S., Peixoto, J., Bessada, S., Pimentel, F.B., et al., 2020. Pigments content (chlorophylls, fucoxanthin and phycobiliproteins) of different commercial dried algae. Separations 7 (2). https://doi.org/10.3390/separations7020033.

[34] Stengel, D.B., Connan, S., 2015. Natural products from marine algae. Preface. Methods Mol Biol 1308, v–vii.

[35] Huang, Y., Adeleye, A.S., Zhao, L., Minakova, A.S., Anumol, T., Keller, A.A., 2019. Antioxidant response of cucumber (*Cucumis sativus*) exposed to nano copper pesticide: Quantitative determination via LC-MS/MS. Food Chem 270, 47–52. https://doi.org/10.1016/j.foodchem.2018.07.069.

[36] Pang, Z., Zhou, G., Ewald, J., Chang, L., Hacariz, O., Basu, N., et al., 2022. Using MetaboAnalyst 5.0 for LC-HRMS spectra processing, multi-omics integration and covariate adjustment of global metabolomics data. Nat Protoc 17 (8), 1735–1761. https://doi.org/10.1038/s41596-022-00710-w.

[37] Xia, J., Wishart, D.S., 2011. Web-based inference of biological patterns, functions and pathways from metabolomic data using MetaboAnalyst. Nat Protoc 6 (6), 743–760. https://doi.org/10.1038/nprot.2011.319.

[38] Jung, Y., Ahn, Y.G., Kim, H.K., Moon, B.C., Lee, A.Y., Ryu, D.H., et al., 2011. Characterization of dandelion species using $^{1}$H NMR- and GC-MS-based metabolite profiling. Analyst 136 (20), 4222–4231. https://doi.org/10.1039/c1an15403f.

[39] Chong, J., Wishart, D.S., Xia, J., 2019. Using metaboanalyst 4.0 for comprehensive and integrative metabolomics data analysis. Curr Protoc Bioinforma 68 (1), e86. https://doi.org/10.1002/cpbi.86.

[40] Pickhardt, P.C., Fisher, N.S., 2007. Accumulation of inorganic and methylmercury by freshwater phytoplankton in two contrasting water bodies. Environ Sci Technol 41 (1), 125–131. https://doi.org/10.1021/es060966w.

[41] Garcia-Calleja, J., Cossart, T., Pedrero, Z., Santos, J.P., Ouerdane, L., Tessier, E., et al., 2021. Determination of the intracellular complexation of inorganic and methylmercury in cyanobacterium *Synechocystis* sp. PCC 6803. Environ Sci Technol 55 (20), 13971–13979. https://doi.org/10.1021/acs.est.1c01732.

[42] Mason, R.P., Reinfelder, J.R., Morel, F.M.M., 1995. Bioaccumulation of mercury and methylmercury. Water Air Soil Poll 80 (1-4), 915–921. https://doi.org/10.1007/Bf01189744.

[43] Mason, R.P., Reinfelder, J.R., Morel, F.M.M., 1996. Uptake, toxicity, and trophic transfer of mercury in a coastal diatom. Environ Sci Technol 30 (6), 1835–1845. https://doi.org/10.1021/es950373d.

[44] Moye, H.A., Miles, C.J., Phlips, E.J., Sargent, B., Merritt, K.K., 2002. Kinetics and uptake mechanisms for monomethylmercury between freshwater algae and water. Environ Sci Technol 36 (16), 3550–3555. https://doi.org/10.1021/es011421z.

[45] Kotyk, A., Struzinsky, R., 1977. Effect of high substrate concentrations on active transport parameters. Biochim Biophys Acta 470 (3), 484–491. https://doi.org/10.1016/0005-2736(77)90139-0.

[46] Rezayian, M., Niknam, V., Ebrahimzadeh, H., 2019. Oxidative damage and antioxidative system in algae. Toxicol Rep 6, 1309–1313. https://doi.org/10.1016/j.toxrep.2019.10.001.

[47] Szivak, I., Behra, R., Sigg, L., 2009. Metal-induced reactive oxygen species production in *Chlamydomonas reinhardtii* (Chlorophyceae). J Phycol 45 (2), 427–435. https://doi.org/10.1111/j.1529-8817.2009.00663.x.

[48] Tang, W., He, M., Chen, B., Ruan, G., Xia, Y., Xu, P., et al., 2023. Investigation of toxic effect of mercury on *Microcystis aeruginosa:* Correlation between intracellular mercury content at single cells level and algae physiological responses. Sci Total Environ 858 (Pt 2), 159894. https://doi.org/10.1016/j.scitotenv.2022.159894.

[49] Mallick, N., Mohn, F.H., 2003. Use of chlorophyll fluorescence in metal-stress research: a case study with the green microalga *Scenedesmus*. Ecotoxicol Environ Saf 55 (1), 64–69. https://doi.org/10.1016/s0147-6513(02)00122-7.

[50] Sathasivam, R., Ki, J.S., 2019. Differential transcriptional responses of carotenoid biosynthesis genes in the marine green alga *Tetraselmis suecica* exposed to redox and non-redox active metals. Mol Biol Rep 46 (1), 1167–1179. https://doi.org/10.1007/s11033-018-04583-9.

[51] Gregoire, D.S., Poulain, A.J., 2014. A little bit of light goes a long way: the role of phototrophs on mercury cycling. Metallomics 6 (3), 396–407. https://doi.org/10.1039/c3mt00312d.

[52] Ge, Y.H., Liu, X.D., Nan, F.R., Liu, Q., Lv, J.P., Feng, J., et al., 2022. Toxicological effects of mercuric chloride exposure on *Scenedesmus quadricauda*. Water 14 (20), 3228. https://doi.org/10.3390/w14203228.

[53] Bezzubova, E.M., Drits, A.V., Mosharov, S.A., 2018. Effect of mercury chloride on the chlorophyl and pheophytin content in marine microalgae: measuring the flow of autotrophic phytoplankton using sediment traps data. Oceanology 58 (3), 479–486. https://doi.org/10.1134/S0001437018030037.

[54] Protopopov, F.F., Matorin, D.N., Seifullina, N.H., Bratkovskaya, L.B., Zayadan, B. K., 2015. Effect of methylmercury on the light dependence fluorescence parameters in a green Alga *Chlamydomonas moewusii*. Mikrobiologiia 84 (6), 725–731. https://doi.org/10.1134/s0026261715060119.

[55] Beauvais-Fluck, R., Slaveykova, V.I., Cosio, C., 2016. Transcriptomic and physiological responses of the green microalga chlamydomonas reinhardtii during short-term exposure to subnanomolar methylmercury concentrations. Environ Sci Technol 50 (13), 7126–7134. https://doi.org/10.1021/acs.est.6b00403.

[56] Gojkovic, Z., Skrobonja, A., Funk, C., Garbayo, I., Vílchez, C., 2022. The role of microalgae in the biogeochemical cycling of methylmercury (MeHg) in aquatic environments. Phycology 2 (3), 344–362. https://doi.org/10.3390/phycology2030019.

[57] Luengen, A.C., Fisher, N.S., Bergamaschi, B.A., 2012. Dissolved organic matter reduces algal accumulation of methylmercury. Environ Toxicol Chem 31 (8), 1712–1719. https://doi.org/10.1002/etc.1885.

[58] Keck, F., Bouchez, A., Franc, A., Rimet, F., 2016. Linking phylogenetic similarity and pollution sensitivity to develop ecological assessment methods: a test with river diatoms. J Appl Ecol 53 (3), 856–864. https://doi.org/10.1111/1365-2664.12624.

[59] Bromke, M.A., 2013. Amino Acid biosynthesis pathways in diatoms. Metabolites 3 (2), 294–311. https://doi.org/10.3390/metabo3020294.

[60] Vallon, O., Spalding, M.H., 2009. Amino acid metabolism, The Chlamydomonas Sourcebook. Elsevier, pp. 115–158.

[61] Less, H., Galili, G., 2008. Principal transcriptional programs regulating plant amino acid metabolism in response to abiotic stresses. Plant Physiol 147 (1), 316–330. https://doi.org/10.1104/pp.108.115733.

[62] Allen, A.E., Dupont, C.L., Obornik, M., Horak, A., Nunes-Nesi, A., McCrow, J.P., et al., 2011. Evolution and metabolic significance of the urea cycle in photosynthetic diatoms. Nature 473 (7346), 203–207. https://doi.org/10.1038/nature10074.

[63] Obata, T., Fernie, A.R., Nunes-Nesi, A., 2013. The central carbon and energy metabolism of marine diatoms. Metabolites 3 (2), 325–346. https://doi.org/10.3390/metabo3020325.

[64] Stepansky, A., Leustek, T., 2006. Histidine biosynthesis in plants. Amino Acids 30 (2), 127–142. https://doi.org/10.1007/s00726-005-0247-0.

[65] Lieberman, M.A., Ricer, R.E., 2020. Biochemistry, molecular biology, and genetics. Wolters Kluwer.

[66] Hildebrandt, T.M., Nunes Nesi, A., Araujo, W.L., Braun, H.P., 2015. Amino acid catabolism in plants. Mol Plant 8 (11), 1563–1579. https://doi.org/10.1016/j.molp.2015.09.005.

[67] Szabados, L., Savoure, A., 2010. Proline: a multifunctional amino acid. Trends Plant Sci 15 (2), 89–97. https://doi.org/10.1016/j.tplants.2009.11.009.

[68] Matysik, J., Alia, Bhalu, B., Mohanty, P., 2002. Molecular mechanisms of quenching of reactive oxygen species by proline under stress in plants. Curr Sci India 82 (5), 525–532.

[69] Taylor, N.L., Heazlewood, J.L., Day, D.A., Millar, A.H., 2004. Lipoic acid-dependent oxidative catabolism of alpha-keto acids in mitochondria provides evidence for branched-chain amino acid catabolism in Arabidopsis. Plant Physiol 134 (2), 838–848. https://doi.org/10.1104/pp.103.035675.

[70] Liang, Y., Kong, F., Torres-Romero, I., Burlacot, A., Cuine, S., Legeret, B., et al., 2019. Branched-chain amino acid catabolism impacts triacylglycerol homeostasis in chlamydomonas reinhardtii. Plant Physiol 179 (4), 1502–1514. https://doi.org/10.1104/pp.18.01584.

[71] Binder, S., Knill, T., Schuster, J., 2007. Branched-chain amino acid metabolism in higher plants. Physiol Plant 129 (1), 68–78. https://doi.org/10.1111/j.1399-3054.2006.00800.x.

[72] Xu, J.J., Fang, X., Li, C.Y., Yang, L., Chen, X.Y., 2020. General and specialized tyrosine metabolism pathways in plants. aBIOTECH 1 (2), 97–105. https://doi.org/10.1007/s42994-019-00006-w.

[73] Antonacci, A., Lambreva, M.D., Margonelli, A., Sobolev, A.P., Pastorelli, S., Bertalan, I., et al., 2018. Photosystem-II D1 protein mutants of *Chlamydomonas*

*reinhardtii* in relation to metabolic rewiring and remodelling of H-bond network at Q(B) site. Sci Rep 8 (1), 14745. https://doi.org/10.1038/s41598-018-33146-y.
[74] Lohr, M., 2009. Carotenoids. In: Elizabeth, H.Harris, Stern, David B., George, B. Witman (Eds.), The Chlamydomonas Sourcebook. Academic Press, London, pp. 799–817. https://doi.org/10.1016/b978-0-12-370873-1.00029-0.
[75] Lameka, K., Farwell, M.D., Ichise, M., 2016. Positron emission tomography. Handb Clin Neurol 135 209–227. https://doi.org/10.1016/B978-0-444-53485-9.00011-8.
[76] Colovic, M.B., Vasic, V.M., Djuric, D.M., Krstic, D.Z., 2018. Sulphur-containing amino acids: protective role against free radicals and heavy metals. Curr Med Chem 25 (3), 324–335. https://doi.org/10.2174/0929867324666170609075434.
[77] Kroth, P.G., Chiovitti, A., Gruber, A., Martin-Jezequel, V., Mock, T., Parker, M.S., et al., 2008. A model for carbohydrate metabolism in the diatom *Phaeodactylum tricornutum* deduced from comparative whole genome analysis. PloS One 3 (1), e1426. https://doi.org/10.1371/journal.pone.0001426.
[78] Voss, I., Sunil, B., Scheibe, R., Raghavendra, A.S., 2013. Emerging concept for the role of photorespiration as an important part of abiotic stress response. Plant Biol (Stuttg) 15 (4), 713–722. https://doi.org/10.1111/j.1438-8677.2012.00710.x.
[79] Wingler, A., Lea, P.J., Quick, W.P., Leegood, R.C., 2000. Photorespiration: metabolic pathways and their role in stress protection. Philos Trans R Soc B-Biol Sci 355 (1402), 1517–1529. https://doi.org/10.1098/rstb.2000.0712.
[80] Zhang, W., Tan, N.G., Li, S.F., 2014. NMR-based metabolomics and LC-MS/MS quantification reveal metal-specific tolerance and redox homeostasis in *Chlorella vulgaris*. Mol Biosyst 10 (1), 149–160. https://doi.org/10.1039/c3mb70425d.
[81] Avidan, O., Brandis, A., Rogachev, I., Pick, U., 2015. Enhanced acetyl-CoA production is associated with increased triglyceride accumulation in the green alga *Chlorella desiccata*. J Exp Bot 66 (13), 3725–3735. https://doi.org/10.1093/jxb/erv166.
[82] Behzadi Tayemeh, M., Esmailbeigi, M., Shirdel, I., Joo, H.S., Johari, S.A., Banan, A., et al., 2020. Perturbation of fatty acid composition, pigments, and growth indices of *Chlorella vulgaris* in response to silver ions and nanoparticles: a new holistic understanding of hidden ecotoxicological aspect of pollutants. Chemosphere 238, 124576. https://doi.org/10.1016/j.chemosphere.2019.124576.
[83] Foyer, C.H., Noctor, G., 2011. Ascorbate and glutathione: the heart of the redox hub. Plant Physiol 155 (1), 2–18. https://doi.org/10.1104/pp.110.167569.
[84] Grill, E., Loffler, S., Winnacker, E.L., Zenk, M.H., 1989. Phytochelatins, the heavy-metal-binding peptides of plants, are synthesized from glutathione by a specific gamma-glutamylcysteine dipeptidyl transpeptidase (phytochelatin synthase). Proc Natl Acad Sci USA 86 (18), 6838–6842. https://doi.org/10.1073/pnas.86.18.6838.
[85] Wu, Y., Wang, W.X., 2012. Thiol compounds induction kinetics in marine phytoplankton during and after mercury exposure. J Hazard Mater 217-218, 271–278. https://doi.org/10.1016/j.jhazmat.2012.03.024.
[86] Wu, Y., Wang, W.X., 2014. Intracellular speciation and transformation of inorganic mercury in marine phytoplankton. Aquat Toxicol 148, 122–129. https://doi.org/10.1016/j.aquatox.2014.01.005.
[87] Moffatt, B.A., Ashihara, H., 2002. Purine and pyrimidine nucleotide synthesis and metabolism. Arab Book 1, e0018. https://doi.org/10.1199/table0018.
[88] Zulu, N.N., Zienkiewicz, K., Vollheyde, K., Feussner, I., 2018. Current trends to comprehend lipid metabolism in diatoms. Prog Lipid Res 70, 1–16. https://doi.org/10.1016/j.plipres.2018.03.001.
[89] Wichard, T., Gerecht, A., Boersma, M., Poulet, S.A., Wiltshire, K., Pohnert, G., 2007. Lipid and fatty acid composition of diatoms revisited: rapid wound-activated change of food quality parameters influences herbivorous copepod reproductive success. Chembiochem 8 (10), 1146–1153. https://doi.org/10.1002/cbic.200700053.
[90] Mäkinen, K., Elfving, M., Hänninen, J., Laaksonen, L., Rajasilta, M., Vuorinen, I., et al., 2017. Fatty acid composition and lipid content in the copepod Limnocalanus macrurus during summer in the southern Bothnian Sea. Helgol Mar Res 71 (1). https://doi.org/10.1186/s10152-017-0491-1.